

NUMERICAL SIMULATION OF HIGH-SPEED SEPARATION FLOW IN THE AEROSPACE PROPULSION SYSTEMS

E.V. Larina*, I.A. Kryukov, I.E. Ivanov**

*

*** Moscow Aviation Institute (National Research University), Russia**

**** Institute for Problems in Mechanics RAS, Russia**

Keywords: *boundary layer separation, turbulence models, compressible flows*

Abstract

Results of numerical simulation of turbulent flow around a high-speed vehicle are presented in the paper. Performance of several two- and three-equation turbulence models based on RANS approach is studied. Special attention is given to the various versions of the three-equation lag turbulence model. The model contains a relaxation type equation for the non-equilibrium eddy viscosity. In the paper, the results of numerical simulation of three high-speed turbulent flows are considered. The first flow is a turbulent separated flow in supersonic rocket nozzle. The second one is a high-speed flow near compression ramp. In addition, a hypersonic flow near scramjet inlet is calculated. It is shown that the lag turbulence model provides acceptable accuracy in most high-speed flows considered.

1 Introduction

Numerical simulations of the flow in the inlet parts (compression corners) and supersonic flows in nozzles have been conducted. The main feature of these flows is the presence of complex shock-wave structures that interacts with the boundary layers, and the turbulence significantly affects the nature of this interaction. Therefore, the study focuses on the possibility of describing such flows using different turbulence models.

Typically the turbulence is not taken into account during the air inlet design. However, the incoming flow turbulence, the transitional and turbulent boundary layers development

significantly affect the structure of the hypersonic vehicle inlet flow. Inlet should provide the required deceleration to supersonic speed at the combustion chamber entrance via the oblique shocks without leading to a significant total pressure loss. A boundary layer is formed on the forebody and inlet walls, and then it interacts in complicated manner with shocks in the inlet leading to separations. The separations consequently lead to a significant increase in heat loads and resistance, which can not only reduce the hypersonic vehicle effectiveness, but may also lead to structural failure.

Conversely, propulsion nozzle serves to accelerate the flow and produce thrust. The separation of boundary layer in the nozzles causes a similar effect – heating (in case of restricted shock separation, e.g. [5]) and decreased efficiency by reducing the thrust or flow asymmetry and lateral loads appearance. Lateral loads can lead to oscillations, which destroy the nozzle. Nozzles, designed for high altitudes, have reduced thrust due to boundary layer separation during take-off and/or landing. Therefore, it is important to be able to simulate the separated flows with good accuracy for a wide range of ambient pressure ([4, 6]).

2 Mathematical model and method

The method used is described in [2]. The system of Favre-Averaged Navier-Stokes equations in two-dimensional case with continuity and energy equations are solved. The system is closed by two- or three-parameter

turbulence model and supplemented with ideal gas state equation. Sutherland's equation with linear law in case of cold temperature is used for laminar viscosity. Thermal conductivity is similar to viscosity and is defined by a constant Prandtl number. Several parametric models are used in simulation, such as k-ε models with different non-equilibrium and compressibility corrections, low-Reynolds number k-ω model [12], so-called «lag» model [8] (referred as k-ω-μ_t here), and k-ε-μ_t model. The latest consist of two equations of standard k-ε model [7] without compressible dissipation and additional relaxation equation for non-equilibrium turbulent viscosity. The turbulence model is built by analogy with k-ω-μ_t model [8] and the model constant is chosen in range [0.01, 15] in the flat nozzle separated flow problem [4]. It value is 0.75. The additional relaxation equation becomes:

$$\frac{\partial \mu}{\partial t} + \frac{\partial \langle u_i \rangle \mu}{\partial x_i} = c_t \frac{k}{e} (\mu_E - \mu) \quad (1)$$

where $\mu_{tE} = c_\mu \rho k^2 / \varepsilon$ is «equilibrium» viscosity, which is used as an auxiliary variable. Obtained non-equilibrium eddy viscosity is included in the motion and energy equations and turbulent quantities transport equations.

The article summarizes the calculations for those models whose results are most relevant experimental data. Due to less stringent requirements to the grid modeling emphasis is placed on high-Reynolds models.

Equations are solved using a second-order Godunov method in space (away from discontinuities) and in time.

3 Computational results

3.1 Separated flow in a plane nozzle

The first test case is the turbulent flow in a plane nozzle [4] with a boundary layer separation. The half angles of the nozzle supersonic divergent and subsonic convergent cone sections are 11.01° and 27.29° respectively. The nozzle expansion ratio is 1.797. The nozzle throat size R* from symmetry

plane to the wall is 0.0137 m. The transonic part of nozzle contour has radius of curvature equal to 0.625R*. The radius of curvature in the constant-width channel and convergent section of nozzle conjugation region is 2R*. Convergent and divergent sections lengths are the same and equal to 0.0578m. The ambient conditions are normal (pressure Pa=102387.14Pa and temperature Ta=293K). The operating fluid is air (γ=1.4). Nozzle pressure drop n, that is entrance pressure P_{in} divided by ambient pressure P_∞: n=P_{in}/P_∞, changes in experiment.

It is clear that the k-ε-μ_t model is able to predict the static pressure value in separated nozzle flows in a wide range of ambient parameters, including separation point location, recovered pressure after the separation point. The exception is the case of non-steady flow like in fig. 1 with n=1.255. In addition the model correlates with the experiment both for Mach disc length and location.

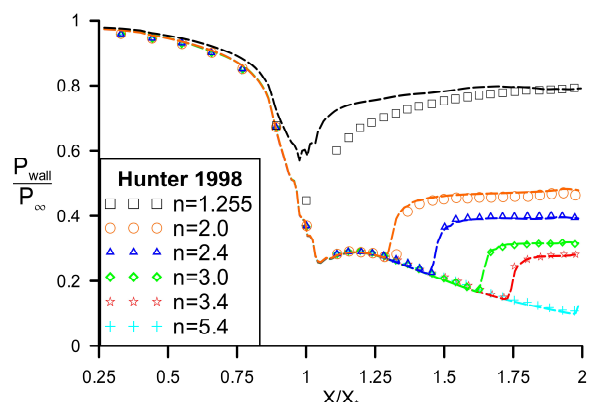


Fig. 1. The nozzle wall static pressure. The curves corresponds to the simulation with k-ε-μ_t model, symbols – to experiment [4].

3.2 Turbulent flow near compression ramp

3.2.1 Supersonic flow near compression ramp (Elfstrom 1972 [1]).

One of the alternatives for air-breathing jet engine configuration is composed of several compression corners with a subsequent isolator. It is necessary to numerically simulate the flow over compression corner for this configuration. For the case presented in fig. 2 the compression corner location is zero. There are four compression corner angles in the experiment:

8°, 16°, 20°, 24° ([10]) and the numerical simulation result with 24° angle is presented in fig. 2. The following incoming flow parameters are: Mach number is 2.85, Reynolds number per 1m is 7.3×10^7 , stagnation pressure is 6.8 atm, stagnation temperature is 268K. There are adiabatic wall conditions, and the horizontal flat plane length is found approximately by momentum thickness $\theta=0.12$ at location - 0.0508m.

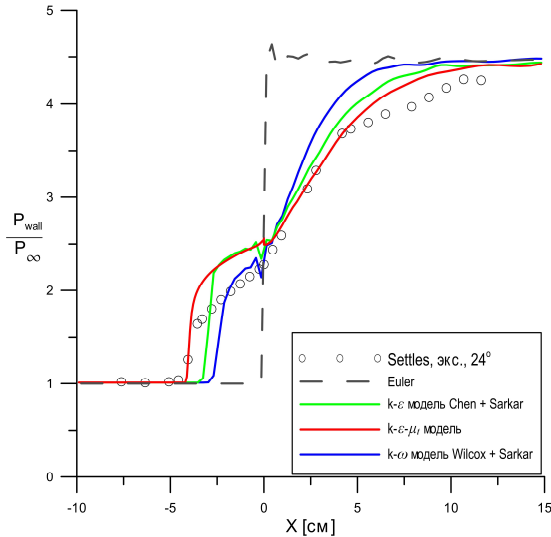


Fig. 2. The compression corner wall static pressure. The curves correspond to the simulation with RANS models (green – model[3] with compressibility correction [9], red - $k-\epsilon-\mu_t$ model, blue - $k-\omega$ model [12] with compressibility correction [9]), symbols – to experiment [10].

In this case the $k-\epsilon-\mu_t$ model accurately predicts the separation point location, but over-predicts pressure “plateau” in the recirculating-reverse flow up to join the mixed layer flowing over this area. Due to significant experimental errors close to interaction, we can assume that there is a reasonable agreement with experiment. Over the distance where the pressure is recovered after the attachment point to the equilibrium boundary layer pressure, $k-\epsilon-\mu_t$ model has the smallest error in comparison with other turbulence models. The numerical simulation recovered pressure is greater than experimental recovered pressure, but it is consistent with non-viscous case value.

Figure 3 shows a transverse velocity profiles comparison between numerical

simulation and experiment (with aligned Mach number field). The dashed line in the figure shows the sonic line within the boundary layer. It is clear that, although it is a good agreement in wall static pressure after the reattachment, transverse parameters still have appreciable error in this region.

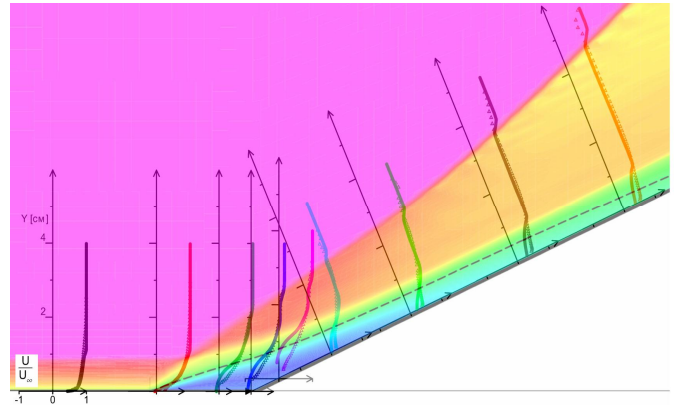


Fig. 3. Two-dimensional picture of the flow over compression corner 24° [10]. Mach number field is aligned with the velocity profiles obtained using the $k-\epsilon-\mu_t$ turbulence model (symbols correspond to the experiment). The velocity is divided by its value in the undisturbed flow.

3.2.2 Supersonic flow near compression and expansion corners configuration (Zhel'tovodov et al. 1987 [13]).

Let's consider another supersonic flow containing compression corner (experiment [13] in mean flow measurement case, the data are taken from [11] database). There are parallel to the incoming flow horizontal plate in the configuration. It continues with small sloped plate 31.3 cm long with 25° incline angle and subsequent horizontal plate which creates local flow expansion. Sloped plate length is 3.22 cm. Incoming flow Mach number is 2.88, Reynolds number per 1m is 3.24×10^7 , stagnation pressure is 4,22 kg/cm², stagnation temperature is 294K. There is adiabatic boundary condition on the walls in simulation. There are supersonic inflow condition on the domain entrance, free outlet boundary condition in the domain top and nonreflecting boundary condition in the domain exit.

The relaxation models results comparison of static pressure is shown in fig. 4. It is clear that low-Reynolds number $k-\omega-\mu_t$ model predict static pressure rise more accurately than the high-Reynolds $k-\varepsilon-\mu_t$ model. The latest underestimates the pressure peak about 20%. The fig. 5 shows static pressure across the flow obtained by $k-\omega-\mu_t$ model and divided by it near wall local value.

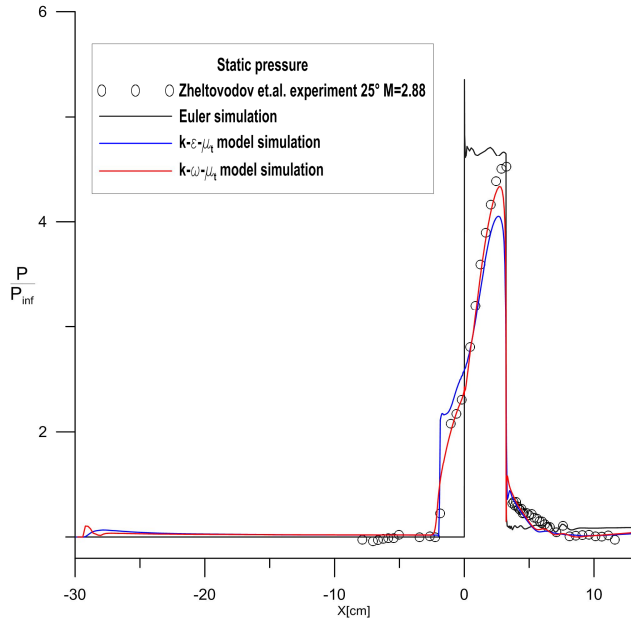


Fig. 4. Static pressure along compression corner wall. The red curve corresponds to $k-\omega-\mu_t$ model, blue - to $k-\varepsilon-\mu_t$ model, symbols – to experiment [13].

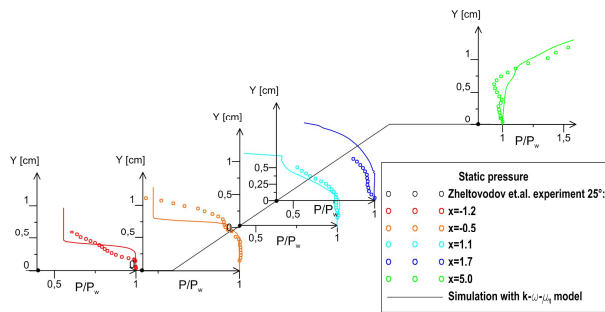


Fig. 5. Static pressure in vicinity of the point of separation. Curves are obtained by $k-\omega-\mu_t$ model. Symbols correspond to experiment [13].

3.2.3 Hypersonic flow near compression and expansion corners configuration (Settles et al. 1979 [13]).

The next test case is hypersonic flow over compression corner with experimental data [1]. There are four experimental angles 15° , 30° , 34° , 38° and the last case is presented as numerical simulation result (fig. 6). Incoming flow and other parameters are following: Mach number 9.22, Reynolds number per 1m is 4.7×10^5 , stagnation temperature 1070K, incident flow temperature 64.5K, wall temperature 295K. Horizontal flat plate length is 56cm (and there is 58cm from computation domain origin to corner location).

This test case is more complicated than the previous one since the interaction region is thinner and pressed into a wall; therefore, parameters gradients are greater in this case. In addition transition region is close to interaction region, and that results in difficulties. Namely, the transition should occur when mixing layer flows above recirculation region. It is seen that the three-equation $k-\varepsilon-\mu_t$ model accurately predicts the static pressure value in recirculation region and leads to a little earlier separation and a little later pressure jump compared with experimental values. Other high-Reynolds model, which described in [3], in contrast, leads to earlier separation and under-predicted pressure jump. The presence of the relaxation equation leads to the length of the pressure recovery over-prediction. The $k-\varepsilon$ model [3] and relaxation equation (1) combination does not improve the results. Even though low-Reynolds models give significantly earlier separation with low static pressure value of the recirculation region on the horizontal plate, reattachment point and recovery region have good agreement with experiment.

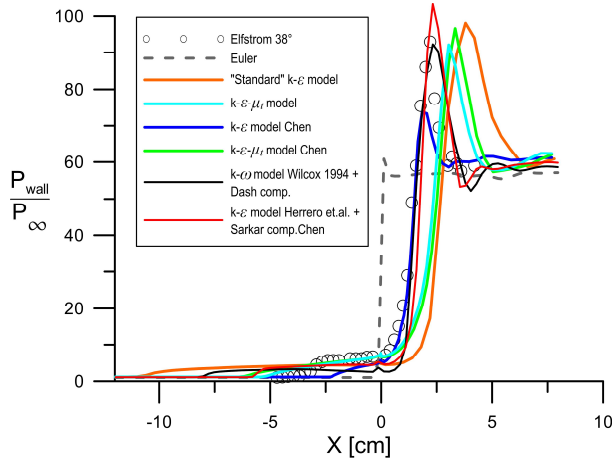


Fig. 6. Wall static pressure for hypersonic flow over compression corner problem. The curves correspond to the simulation with RANS models, symbols – to experiment [1].

3.3 Turbulent flow near hypersonic inlet

The last case considered is a turbulent flow near hypersonic inlet. The inlet is designed for Mach number $M=6$ and angle of attack $\alpha=5^\circ$. Flow conditions are correspond to altitude 30 km. Fig 7 and Fig. 8 show results for $M=6$ and $\alpha=0^\circ$.

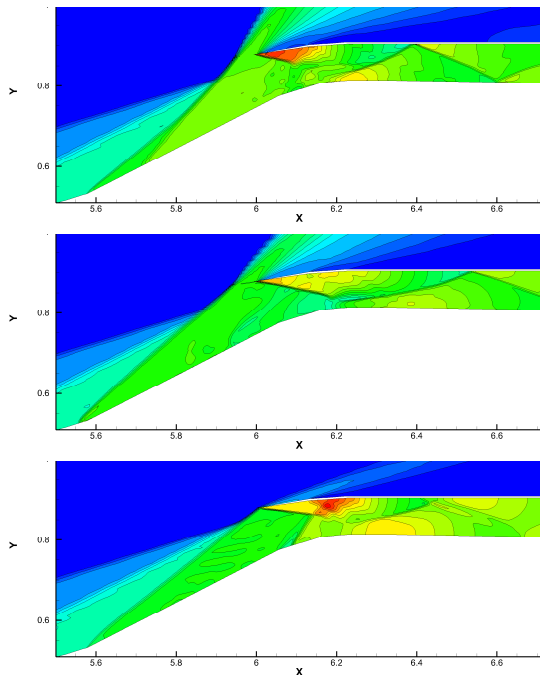


Fig. 7. Static pressure around hypersonic inlet.

On the top part of the figures, the inviscid results are shown. In the middle, the laminar results are shown. The bottom part of these figures corresponds to the computed turbulent flow. Fig. 7 shows the static pressure contour lines and Fig. 8 shows the mass density distributions.

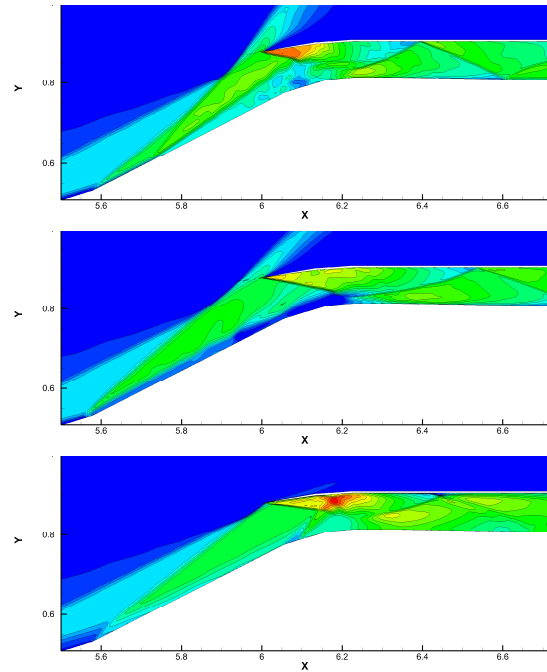


Fig. 8. Contour lines of density around hypersonic inlet.

It can be easily seen that there is noticeable difference in the pressure and density. Shock wave structure inside the inlet is similar, but position, strength and shape are different. The boundary layers on the forebody in the viscous cases change the flow picture just before the inlet.

Conclusions

Results of numerical simulation of high-speed viscous gas flow around vehicle parts are presented. The paper is devoted mainly to comparison of of several two- and three-equation turbulence models based on RANS approach. For the comparison, the results of numerical simulation of three high-speed turbulent flows are considered. These flows are a turbulent separated flow in supersonic rocket nozzle, a high-speed flow near compression

ramp and a hypersonic flow near scramjet inlet model. Special attention is given to the various versions of the three-equation lag turbulence model. It is shown that the developed by authors versions of the lag turbulence model allow to obtain acceptable coincidence with experiment in most high-speed flows considered. The most successful models for separated flow simulation in the compression ramp case are high-Reynolds number $k-\varepsilon$ model [3] with compressibility correction [9], $k-\varepsilon-\mu_t$ model and low-Reynolds number $k-\omega-\mu_t$ («lag») model [8].

References

- [1] Elfstrom G.M. Turbulent Hypersonic Flow at a Wedge-Compression Corner. *J. Fluid Mech.*, 1972, 53, pp 113-127.
- [2] Glushko G. S., Ivanov I. E., Kryukov I. A. Computational method for turbulent supersonic flows. *Matematicheskoe Modelirovanie*, Vol. 21, No. 12, pp. 103-121, 2009. (in Russian)
- [3] Glushko G. S., Ivanov I. E., Kryukov I. A. Turbulence modeling for supersonic jet flows. *Fiziko-himicheskaya kinetika v gazovoy dinamike*, Vol. 9, 2010, www.chemphys.edu.ru/pdf/2010-01-12-023.pdf (in Russian)
- [4] Hunter C.A. Experimental, theoretical, and computational investigation of separated nozzle flows. *AIAA Paper*, 98-3107, 1998.
- [5] Ivanov I.E., Kryukov I.A. Numerical investigations of turbulent flows with free and restricted shock separation. *Vestnik Moskovskogo aviatsionnogo instituta*, Vol. 16, No. 7, pp 23-30, 2009. (in Russian)
- [6] Kryukov I.A., Glushko G.S., Larina E.V. Some peculiarities of turbulence modeling in high-speed flows. *Vestnik of Lobachevsky state university of Nizhni Novgorod*, Vol. 4, pp 902-903, 2011. (in Russian)
- [7] Launder B.E., Spalding D.B. The numerical computation of turbulent flows. *Computer Meth. Appl. Mech. Engr.*, Vol. 3, No. 3, pp 269-289, 1974.
- [8] Olsen M.E., Coakley T. J. The Lag Model, a Turbulence Model for Non Equilibrium Flows. *AIAA Paper*, 2001-2664, 2001.
- [9] Sarkar S., Erlebacher G., Hussaini M.Y., Kreiss H.O. The analysis and modelling of dilatational terms in compressible turbulence. *J. Fluid Mech.*, 227, 473–493, 1991.
- [10] Settles G.S., Fitzpatrick T.J., Bogdonoff S.M. Detailed Study of Attached and Separated Compression Corner Flowfield in High Reynolds Number Supersonic Flow. *AIAA Journal*, Vol. 17, No. 6, 1979.
- [11] Settles G. S., Dodson L.J. Hypersonic Shock/Boundary-Layer Interaction Database. *NASA CR 177577*, 1991.
- [12] Wilcox D. *Turbulence Modeling for CFD*. DCW Industries, Inc., Griffin Printing, Glendale, California, 1994.
- [13] Zheltovodov A.A., Trofimov E.G., Yakovlev V.N. Investigation of Heat Transfer and Turbulence in Supersonic Separation. *ITPM Preprint 22-87*, 1987.

Copyright Statement

The authors confirm that they, and/or their company or organization, hold copyright on all of the original material included in this paper. The authors also confirm that they have obtained permission, from the copyright holder of any third party material included in this paper, to publish it as part of their paper. The authors confirm that they give permission, or have obtained permission from the copyright holder of this paper, for the publication and distribution of this paper as part of the ICAS 2014 proceedings or as individual off-prints from the proceedings.